JOURNAL OF CATALYSIS 151, 125–134 (1995)

Pumice-Supported Pd–Pt Bimetallic Catalysts: Synthesis, Structural Characterization, and Liquid-Phase Hydrogenation of 1,3-Cyclooctadiene

Giulio Deganello,*,†,[1] Dario Duca,* Leonarda F. Liotta,* Antonino Martorana,† Anna Maria Venezia,† Alvise Benedetti,‡ and Giuliano Fagherazzi‡

*Istituto di Chimica e Tecnologia dei Prodotti Naturali del CNR, and †Dipartimento di Chimica Inorganica dell'Università, Via Archirafi 26-28, 90123 Palermo, Italy; and ‡Dipartimento di Chimica Fisica dell'Università di Venezia, Calle Larga S. Marta 2137, 30123 Venice, Italy

Received December 20, 1993; revised March 25, 1994

A series of pumice-supported palladium–platinum bimetallic catalysts were prepared and investigated by X-ray scattering (WAXS and SAXS) and XPS techniques. An alloy Pd–Pt was formed. The less abundant metal was found to segregate to the surface. The catalysts were tested in the liquid-phase hydrogenation of 1,3-cyclooctadiene to cyclooctene, and compared with similarly prepared pumice-supported palladium and platinum catalysts and other supported Pd–Pt catalysts reported in the literature. The addition of platinum reduces the activity and the selectivity of the palladium catalysts. Differences between the activity of these pumice-supported catalysts and the activity of previously described Pd and Pd–Pt catalysts on other supports, are attributed to the presence, in the latter, of diffusional processes.

1. INTRODUCTION

Supported palladium catalysts are very active in the semihydrogenation of alkadienes and alkynes (1–3). Correlation between particle sizes and activity and/or selectivity is still controversial (4–6); a decrease of the specific activity with increasing Pd dispersion is usually found (6, 7). This trend is partially modified with pumice-supported palladium catalysts (8); the specific activity in the liquid phase hydrogenation of 1,3-cyclooctadiene (1,3-COD) to cyclooctene (COE) is practically constant up to dispersion (D_x) ~35% and decreases slowly at higher dispersions. This behaviour has been attributed to the presence of alkali metal ions which, through electron-donating alkali metal–oxygen composites, induce a higher electron density on palladium particles supported on pumice, as detected by XPS (9) and Auger spectroscopy (10) studies. The increased electron density should decrease the strength of the diene–metal interaction and promote the hydrogenation of 1,3-COD (8). The positive effects of the electron donation are counterbalanced by the progressive loss of metallic character (7) occurring at higher dispersions. However, the decrease of activity is quite smaller than that found in Pd catalysts on other supports. A migration of alkali metal ions on the electron-rich Pd surface, diminishing the ensemble size, could be an alternative or additional explanation for the above trend of activity. The decrease of activity at higher dispersion has been recently proved to be due to excessive electron density on the smaller metallic particles.

The structure of pumice, an amorphous aluminosilicate consisting of linked tetrahedral SiO_4 units with about one in ten units being replaced by aluminate, AlO_4^-, has been studied by XPS and ^{27}Al MAS NMR (11) and by neutron diffraction (12).

The structural study by X-ray analysis of supported metal catalysts with low metal concentration is difficult (13), because of X-ray scattering interferences between the metal particles and the support (14). However, with a support like pumice these interferences are minimized (15, 16), owing to its low surface area (about 5 m^2/g) and low microporosity, so that structural parameters can also be easily obtained with low metal loading (17). Moreover, we have shown (8) that, in the hydrogenation of dienes, pumice-supported palladium catalysts have activity and selectivity comparable with and sometimes better than those presented by palladium on other supports of great surface area (18). Therefore, the influence of the surface area of an inert support in determining the activity and selectivity of a supported metal catalyst is not important, at least at low metal concentration, which is the more interesting case for industrial purposes. Besides, a low surface area of the support minimizes the effects of intraparticle mass and heat transfer and allows kinetic studies of catalyzed reactions on the basis of a pure chemical regime (8), providing that other diffusional processes are not important.

Highly dispersed pumice-supported palladium cata-

[1] To whom correspondence should be addressed.

0021-9517/95 $6.00

lysts have been obtained (17) by reacting [Pd(η^3-C_3H_5)$_2$] (18) with surface -OH groups of pumice and then reducing the anchored Pd–allyl species with hydrogen following a procedure described by Yermakov (19) and used for vitreous supports (20, 21). The use of Pt–allyl derivatives (22) allowed the preparation of similar pumice-supported platinum catalysts (23). Pt catalysts showed, as expected (24), lower activity and selectivity, in the hydrogenation of 1,3-COD, than the palladium ones.

The catalystic properties of a supported transition metal can be altered by the addition of a second transition metal (25) and improvement of selectivity has been obtained by the incorporation of a second metal (2, 26–28) in supported Pd catalysts. The increasing interest in supported bimetallic catalysts (25–30) prompted us to prepare and structurally characterize a series of pumice-supported Pd–Pt catalysts and to test them in the liquid-phase hydrogenation of 1,3-COD to COE. This work aimed to improve the performance of the previously reported pumice-supported Pd catalysts (8, 17) by employing a suitable Pd–Pt alloy, since it was reported that Pd–Pt catalysts on vitreous synthetic aluminosilicates (31) in comparison with analogous Pd catalysts present some advantages in the liquid-phase hydrogenation of phenylacetylene.

2. EXPERIMENTAL

All the employed reagents had an analytical grade. Solvents (Riedel de Haën or Aldrich) were dried and distilled from potassium, under nitrogen atmosphere, before use.

1,3-COD (Aldrich) was purified by fractional distillation from potassium, passed over activated alumina, and stored at −5°C in nitrogen. Purity was checked by GC analysis.

Hydrogen of high purity of GC (ISO SpA, Palermo) was passed through a BTS catalyst (Fluka) to remove traces of oxygen. All the reactions, except those carried out in hydrogen, were performed in atmosphere of purified nitrogen or argon.

The preliminary treatment of pumice powder (by Pumex SpA, Lipari) used as support has been reported previously (17).

[Pd(η^3-C_3H_5)$_2$] (18) and [Pt(η^3-C_3H_5)$_2$] (22) were prepared according to published procedures.

2.1. Catalyst Synthesis

Anchorage of the allyl derivatives to the hydroxyl groups of pumice was carried out following a procedure derived from Yermakov (19) and used for the preparation of pumice-supported Pd catalysts (17).

Pentane solutions of [Pd(η^3-C_3H_5)$_2$] and [Pt(η^3-C_3H_5)$_2$] in various ratios were added to a pumice suspension in pentane (15 g in 75 ml) at −5°C and the mixture was magnetically stirred for 1 h. The mixture was then stirred at 10°C for 30 min to ensure complete reaction. The solution containing residual allyl complexes was syringed out and replaced with pure pentane until the solvent was colorless, to avoid formation of bulk metal derived from unreacted allyl complexes in the successive reduction (17). Reduction with high-purity hydrogen was accomplished at −10°C for 30 min and then at room temperature for 1 h. Most of the solvent was syringed out and the residual solvent was pumped away at 0°C. The catalyst was dried in vacuum at room temperature and stored in nitrogen containing traces of oxygen.

2.2. Catalytic Hydrogenation

The hydrogenation of 1,3-COD was performed in a mechanically stirred tank reactor (8) operating in batch conditions. Tests to avoid the presence of diffusional processes of hydrogen were performed with the most active catalyst (Pd_{100}). The reactor and the procedure were already reported (8). Before starting the hydrogenation, the suspension of the catalyst in THF was stirred for 30 min with the diolefin or with H_2 ("diolefin or hydrogen preconditioning").

All reactions were performed at a constant stirring of 2500 rpm. The diolefin/palladium molar ratio was 10,000 : 1 and the diolefin concentration in THF was 0.25 *M*.

The above catalytic hydrogenations were carried out also with magnetic stirring (nominal 1000 rpm; all other conditions were the same as outlined in the case of mechanical stirring [2500 rpm]). Experiments performed with the mechanical stirring, at different but controlled rpm, show that the activity data obtained with the nominal magnetic stirring of 1000 rpm are equivalent to those obtained with our mechanical stirring of 200 rpm.

2.3. Kinetic Analysis

Kinetic analyses were performed by a GC Dani 3800 HR PTV equipped with a Supelco capillary column SPB 1701 and with a Dani 68/10 FID detector. The system was linked to a Shimadzu C-RIB Chromatopac automatic integrator. The results obtained in repeated experiments showed deviation smaller than 5%.

2.4. X-Ray Analysis

In order to evaluate the average crystallite size of the metallic phase a line-broadening X-ray diffraction analysis (WAXS-LB) was carried out according to previously reported best-fitting procedures (17, 32). Owing to the very broad and weak peaks diffracted by the metallic phase only the 111 reflection could be investigated. From the so-obtained optimized parameters of the best-fitted

pseudo-Voigt functions describing the $K\alpha_1$–$K\alpha_2$ components of this reflection a single-peak Fourier analysis was performed by attributing the observed LB to crystallite smallness only (after having eliminated the instrumental broadening) (17). In such a way a volume-weighted crystallite size, $\langle D\rangle_{WAXS}$, as measured perpendicularly to the (111) crystallographic planes, was obtained. This procedure is equivalent to employing the Scherrer equation starting from the integral breadth, but with the Fourier analysis the instrumental broadening can be eliminated with higher accuracy.

For this analysis we used a vertical powder diffractometer equipped with a focusing graphite monochromator on the diffracted beam. Ni-filtered Cu$K\alpha$ radiation was employed. The profile intensities were measured step by step (0.05° in 2θ) in several runs for a whole fixed time of 150 s using a high stability generator operating at 40 kV and 30 mA. The diffractograms were taken in the range 30–60° in 2θ.

The corresponding metal hydride diffractograms were obtained by *in situ* diffraction experiments carried out at 25°C by using a special sample holder where a flux of pure hydrogen was allowed to enter and overflow (33). The holder was sealed with a very thin Kapton sheet. The measurement of 2θ was calibrated using a standard Pd powder (15) irradiated under the same experimental conditions (edge a_0, of the *fcc* unit cell: 3.8898 Å).

SAXS data were collected with a Paar compact Kratky camera, using Ni-filtered $K\alpha$ radiation and a scintillator counter, with fixed 10^5 counts per angular abscissa. The specific surface S_{Sp} of the metal, the Porod average diameter (surface-weighted), D_p, and the diameter (volume-weighted), $\langle D\rangle_{SAXS}$, averaged on the metal particle size distribution, calculated with a suitable Titchmarsch transform, were determined according to previous work (17, 34). The percentage of metallic atoms exposed, D_x, was determined from D_p on the basis of the published values (35) concerning the numbers of surface metal atoms per polycrystalline surface unit area in the proper ratio obtained by XPS surface analyses (9).

2.5. *XPS Analysis*

XPS analyses were performed with a Vacuum Generators ESCALAB Mk II spectrometer equipped with an X-ray source of aluminum (Al$K\alpha$ 1486.6 eV). The electron analyzer operated in the fixer analyzer transmission (FAT) mode with pass energy of 20 eV. The calibration of the instrument and the procedure of data analysis have been described previously (9).

3. RESULTS AND DISCUSSION

The synthesis of Pd and Pt catalysts via the corresponding diallyl derivatives has been applied to the preparation of mixed Pd–Pt catalysts. The reduction under mild conditions of the molecular species on the surface of pumice probably produces single atoms forming metal particles with small dimensions.

The list of the catalysts investigated in this work is reported in Table 1, together with the dimensions D_p,

TABLE 1

Chemical, Structural, and Surface Characterizations of the Metal Phase

Catalyst	% Met.[a]	Pd(wt%)	%at.Pd[b]	D_p[c]	$\langle D\rangle_{SAXS}$[d]	$\langle D\rangle_{WAXS}$[d]	D_x(%)[f]	$(Pd/Pt)_{XPS}$	$(Pd/Pt)_{bulk}$	Segr.%[g]	I_1/I_2[h]
Pd_{100}	0.61	0.61	1.00	35	32	27	32	—	—	—	0.39
$Pd/Pt_{99/1}$	0.55	0.54	0.99	24	37	27	47	n.d.	n.d.	n.d.	0.50
$Pd/Pt_{95/5}$	0.54	0.51	0.97	32	41	42	35	13.20	31.70	+58.3	0.40
$Pd/Pt_{90/10}$	0.52	0.47	0.95	45	61	24	25	7.00	17.30	+59.3	0.37
$Pd/Pt_{3/1}$	0.69	0.48	0.81	38	42	28	29	4.00	4.16	+3.8	0.35
$Pd/Pt_{2/2}$	0.43	0.22	0.66	36	44	35	31	1.65	1.81	+8.8	0.35
$Pd/Pt_{1/3}$	0.54	0.16	0.44	27	37	50	41	1.02	0.80	−27.5	0.36
$Pd/Pt_{10/90}$	0.75	0.08	0.18	25	34	52	45	0.31	0.21	−47.6	0.25[i]
Pt_{100}	0.66	—	0.00	28	39	53	40	—	—	—	

[a] Total metal content (wt.%, i.e., grams of Pd + Pt per 100 g of catalysts).

[b] Atomic percentage of Pd by chemical analysis.

[c] Porod diameter from SAXS measurements, in Ångstroms.

[d] Average particle diameter obtained from SAXS by the Titchmarsch transform, in Ångstroms.

[e] Apparent average Pd–Pt crystallite diameters obtained by LB-WAXS measurements, in Ångstroms.

[f] Dispersion of the metallic phase, from D_p.

[g] Calculated as % variation of the superficial value respect to the bulk: $[(Pd/Pt)_{bulk} - (Pd/Pt)_{XPS}/(Pd/Pt)_{bulk}]\%$.

[h] Normalized XPS intensity ratios $I(Pd\ 3d_{3/2})/I(Pd\ MNN)$ for various catalysts (for pure metal foil $I_1/I_2 = 0.26$) are calculated as outlined in Ref. (9). The values are different from the previously reported ones (9) because here SAXS-derived dimensions rather than WAXS-derived dimensions have been used.

[i] The error in this measurement is ±20% owing to the very low palladium loading. The error for the other samples is ±10%.

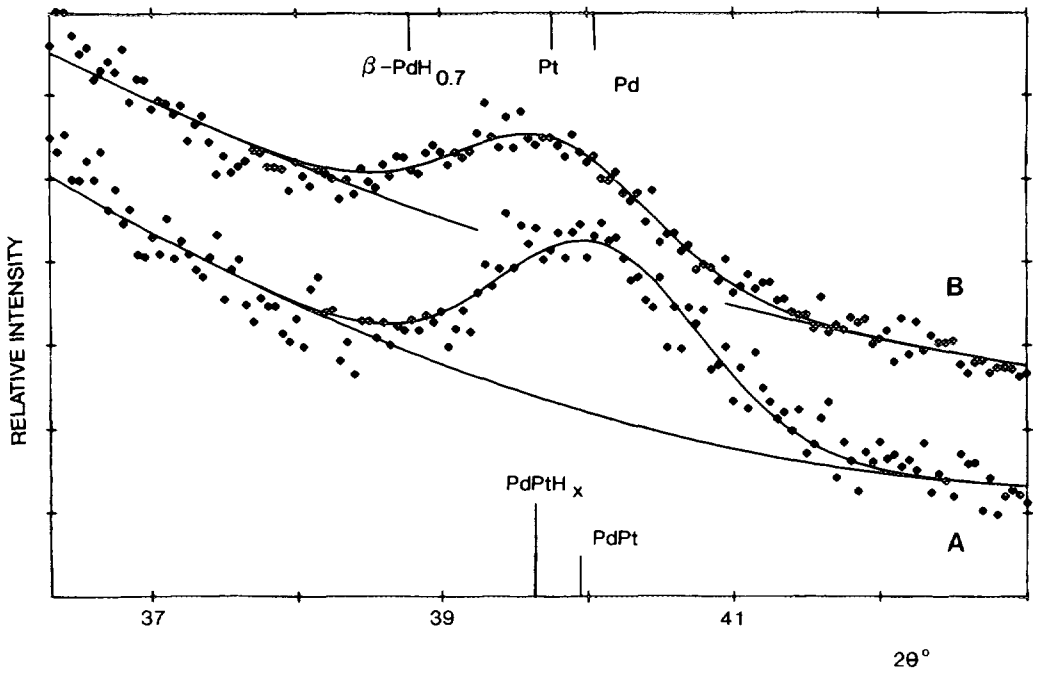

FIG. 1. WAXS measurements upon hydrogen absorption. Formation of Pd–Pt alloy documented by the shift, upon hydrogen absorption, of the 111 WAXS reflection of the Pd–Pt1/3 catalyst (plot A) with respect to the corresponding reflection of the same catalyst (plot B). In the upper part of the figure framework the angular positions obtained from the corresponding JCPDS data are reported. In the lower part the peak maxima positions obtained by the fitting procedure for the catalyst are shown.

$\langle D\rangle_{SAXS}$, and $\langle D\rangle_{WAXS}$ of metal particles and crystallites determined by SAXS and WAXS analyses, the corresponding metal particle dispersion D_x, the total metal content (wt%), and the atomic percentage of palladium in the metal phase derived by chemical analyses (36). Data from XPS analyses are also included.

By inspection of Table 1, it can be noted that the agreement among particle and crystallite sizes is fairly good, within the known errors of the two techniques (±15%), except for the last three (more rich in Pt) specimens. For these specimens a systematically larger value for the size of the metal domains, as determined by WAXS-line broadening, with respect to the particle sizes obtained by SAXS, was detected. This evidence is in contrast with the usually found relations $\langle D\rangle_{SAXS} > D_p > \langle D\rangle_{WAXS}$; the discrepancy is probably due to a large fraction of very small crystallites or clusters whose contribution to the WAXS scattering is merged with the amorphous background of the support. As a consequence of the greater sensitivity of SAXS to very dispersed and very small amounts of scattering matter, the D_p values should be considered, in our opinion, more reliable than the $\langle D\rangle_{WAXS}$ values determined by WAXS and therefore the metal dispersions D_x were calculated from D_p.

It is well known that palladium and platinum metals are completely miscible over the full range of composition (27). The formation of alloy in our pumice-supported Pd–Pt catalysts is documented on the basis of a decreased shift (towards lower 2θ Bragg angles) of the 111 peak in WAXS patterns of Pd–Pt catalysts, upon hydrogen adsorption, with respect to the corresponding shift due to hydride phase β-$PdH_{0.7}$ (see Fig. 1, where, for example, the hydride formation in the Pd–$Pt_{1/3}$ sample is reported). It is worth noting that a pronounced crystallite size smallness (<50 Å) of Pd could also give a progressively lower adsorption of hydrogen in the *fcc* palladium phase, as observed by many authors (37–39). On the basis of a systematic research work on the hydride formation in pure Pd catalysts having very high dispersions (40), we have concluded that, in all samples here investigated, the observed shift decrease, when the particle size effect is taken off, can be related to the formation of a Pd–Pt alloy. The width at half maximum of the 111 reflection has slightly changed under the hydrogen flow, from 1.7 (1)° for the Pd–$Pt_{1/3}$ bimetallic catalyst to 1.9 (1)°. This is another proof of the uniqueness of the crystal phase during the hydrogenation process. This technique has already proved the formation of Pd–Pt alloys in bimetallic catalysts on vitreous supports (41).

A quantitative X-ray photoelectron spectroscopy (XPS) analysis has been made using XPS peak areas of the core levels Pd 3*d* and Pt 4*f* and the photoionization

cross sections given by Scofield (42), corrected by the asymmetry function (43). Pd/Pt atomic ratios have been calculated for each sample (9) and compared with the bulk atomic ratios obtained by chemical analysis. The XPS intensity ratio Pd $3d$/Pt $4f$ (related to the surface atomic concentration) in comparison to the bulk atomic ratio may be indicative of segregation of metal to the surface. The surface ratios (XPS) are almost the same as the bulk ones in the samples richer in platinum, whereas they become smaller than the bulk ones after sample Pd/$Pt_{3/1}$, when palladium content increases (Table 1). In addition the XPS surface atomic concentration of platinum in the bimetallic catalyst Pd/$Pt_{10/90}$, having a platinum loading of 0.67 wt%, was found to be half the platinum concentration in the monometallic Pt catalyst with the same loading of metal. Since the D_p values for the above samples are very close, the smaller XPS platinum concentration in this platinum-rich catalyst could be due to the presence of palladium in the topmost layer.

By exploiting the changes in sampling depths of the electrons with different kinetic energies ejected from different core levels of the same element, it is possible to detect a concentration gradient in the aggregate of metals present in these samples (44), as shown in a previous work (9).

All the Pd $3d_{3/2}$/Pd MNN intensity ratios, listed in Table 1, have been "normalized" with respect to the particle dimensions obtained from SAXS measurements, as explained in the footnote to the table. The smaller values found in the platinum-rich catalysts with respect to the monometallic Pd catalyst and to the palladium-rich catalysts suggest a surface enrichment of palladium in the platinum-rich catalysts (9). The segregation to the surface of alloyed crystallites of the less abundant metal is in accord with a statistical growing of metal crystallites during the reduction of the anchored metal complexes. Segregation of palladium in Pd–Pt alloys has already been found by Auger electron spectroscopy (AES) (45) and on the basis of catalytic methods (46).

Despite the accurate structural characterization of these pumice-supported Pd–Pt catalysts, a correlation between structural characteristics and catalytic activity is difficult. The dominant effect of the addition of Pt to pumice-supported palladium catalysts is a marked decrease of activity and selectivity in the hydrogenation of 1,3-COD. However, the presence of Pt gives some information about the mechanism of hydrogenation. In a previous paper (8) we have shown that the liquid-phase hydrogenation of 1,3-COD with pumice-supported Pd catalysts, at constant pressure of H_2 (1 atm.) and in conditions of pure chemical regime, followed a zero-order kinetics up to relatively very high conversion of 1,3-COD ("pseudo-zero-order kinetics"). Starting from eight reasonable steps and following the procedure of Happel and Sellers (47) with a Fortran program developed by us (8), we found five possible rate determining steps

$$\text{(a)}\quad \text{1,3-COD}^* + H_2 \rightleftharpoons \text{COE}^*$$

$$\text{(b)}\quad H_2^* = \text{1,3-COD} \rightleftharpoons \text{COE}^*$$

$$\text{(c)}\quad 2H^* + \text{1,3-COD} \rightleftharpoons \text{COE}^* + *$$

$$\text{(d)}\quad \text{1,3-COD}^* + 2H^* \rightleftharpoons \text{COE}^* + 2^*$$

$$\text{(e)}\quad \text{1,3-COD}^* + H_2^* \rightleftharpoons \text{COE}^* + *,$$

where the asterisks indicate an adsorbed species or, alone, a vacant adsorption site. Only those steps involving reaction of adsorbed COD (1,3-COD*) with a hydrogen source are compatible with a pseudo-zero-order kinetics. However, owing to the constant pressure of hydrogen, used in that study, it was not possible to make the choice between molecular H_2 [(a) Eley–Rideal mechanism (48)] or adsorbed H_2 [(d) $2H^*$ or (e) H_2^*] as a hydrogen source.

In the case of pumice-supported Pt catalysts the hydrogenation of 1,3-COD gives a first-order kinetics (23) which implies that adsorbed 1,3-COD is not important in the rate-determining step, favouring steps (b) and (c). With Pd–Pt catalysts the kinetic data agree again with steps (a), (d), and (e). In this case an induction period is noted when hydrogenation is performed with "diolefin preconditioning," suggesting that the importance of molecular H_2, if any, is not relevant to the reaction mechanism. Moreover, the induction period, already observed with "hydrogen preconditioning" for pumice-supported Pd catalysts (8), is also found with the Pd–Pt catalysts, whereas it is absent with pure Pt catalyst. These results confirm the importance of activated COD (1,3-COD*) in the reactions catalyzed by Pd and Pd–Pt bimetallic catalysts and the irrelevance of that species with Pt catalysts. On the basis of the above discussion the rate-determining step of the hydrogenation of 1,3-COD to COE with pumice-supported Pd–Pt catalysts should be step (d)

$$\text{COD}^* + 2H^* \rightarrow \text{COE}^* + 2^*,$$

the alternative step (e) involving H_2^* being less realistic.

In Fig. 2a some examples of hydrogenation curves are reported. It appears that the experimental data agree well with the theoretical curve (Fig. 2b) obtained by assuming (d) as the rate-determining step.

When we attempt correlation between catalytic activity and structural parameters (Table 2) of pumice-supported Pd–Pt catalysts the only clear indication is that the addition of the second metal reduces drastically the activity. Indeed, the turnover frequency TOF_i calculated with a dispersion which accounts for the total metal content and for the surface enrichment of the metal present

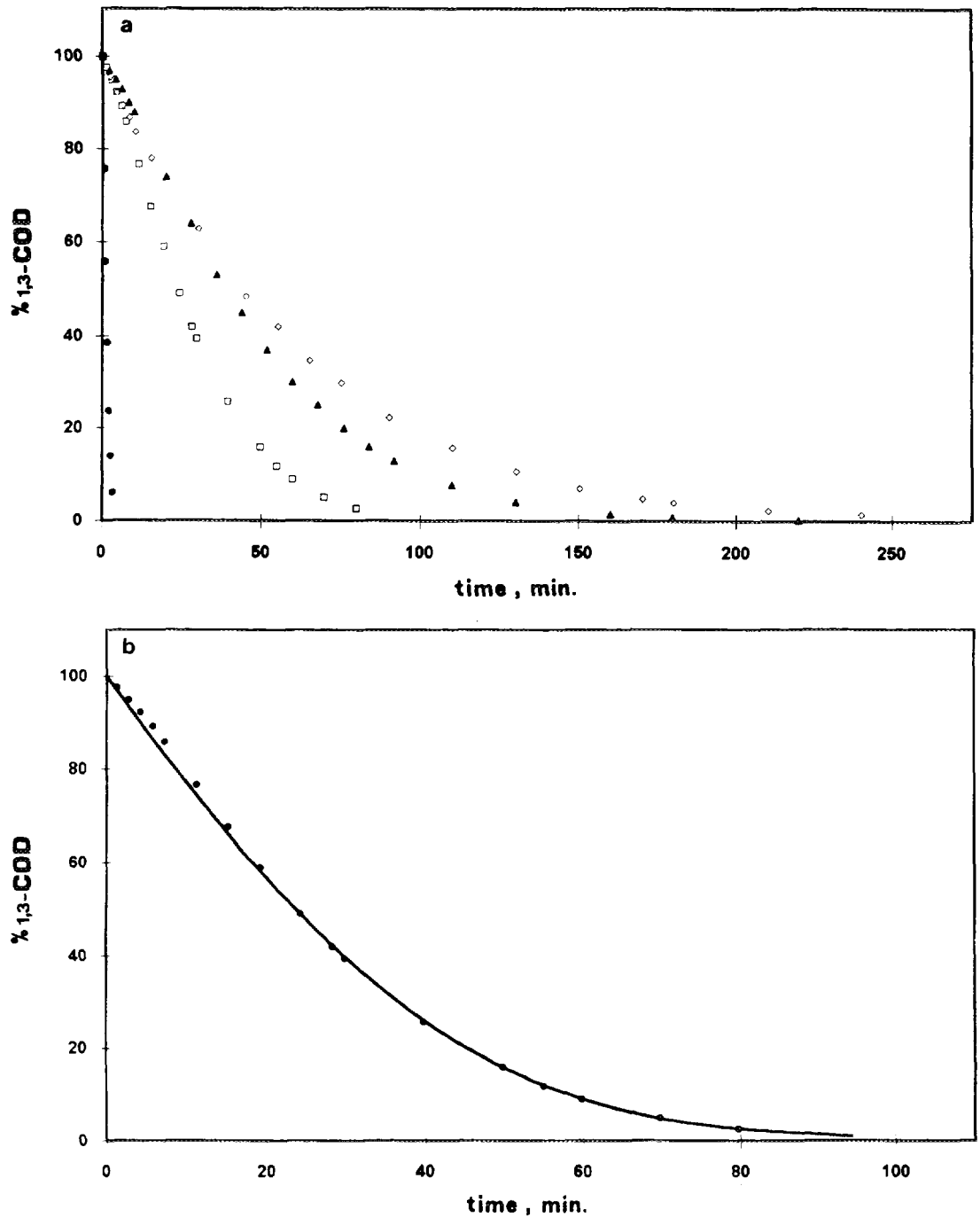

FIG. 2. (a) Experimental points in the hydrogenation of 1,3-COD. The diolefin/M ratio is 10,000 : 1 in the Pd-containing catalysts and 1,250 : 1 in the pure Pt catalyst: (●) Pd_{100}; (□) $Pd-Pt_{90/10}$; (▲) $Pd-Pt_{10/90}$; (◇) Pt_{100}. (b) Example ($Pd-Pt_{90/10}$) of fitting of experimental data with theoretical curve for rate-determining step (d) (see footnote *d* to Table 2 for details on the equation used for fitting).

in minor amount (from XPS data, see Table 1) decreases with the increase of Pt amount (Fig. 3). Another theoretical curve for TOF_1 considers not only the mechanical mixture of the pure Pd and Pt catalysts used in this work at the composition of the alloyed Pd–Pt catalysts, but also the mechanical mixture which accounts for the pure Pd and Pt catalysts with the dimensions corresponding to those found for the alloyed catalysts. While the activity of Pt on pumice is practically constant so that its influence in this curve depends only on the content in Pt, in

TABLE 2

Correlation between Catalytic and Structural Parameters

Catalyst	%Met.[a]	%at.Pd[b]	D_x[c]	$k_1(\times 10^{-1})$[d]	Q[d]	TOF_1[e]	k_1/k_2[f]	S_{90}[g]	S_{100}[h]
Pd_{100}	0.61	1.00	32	172	0.21	90	1214	100	100
$Pd/Pt_{99/1}$	0.55	0.99	47	30	0.22	12	214	100	99.8
$Pd/Pt_{95/5}$	0.51	0.97	35	7.84	0.26	3	90	100	99.0
$Pd/Pt_{90/10}$	0.52	0.94	25	23.9	0.35	17	239	100	99.3
$Pd/Pt_{3/1}$	0.69	0.81	29	14.5	0.35	8	114	98.8	99.2
$Pd/Pt_{2/2}$	0.43	0.64	31	8.79	0.35	3	51	96.6	98.0
$Pd/Pt_{1/3}$	0.54	0.44	41	4.44	0.33	1	50	91.0	96.0
$Pd/Pt_{10/90}$	0.75	0.17	45	14.7	0.40	5	21	88.8	90.0
Pt_{100}	0.66	0.00	40	2.19	n.d.	1	18		87.7

[a] Total metal content (wt.%, i.e., grams of Pd + Pt per 100 g of catalysts).

[b] Atomic percentage of Pd by chemical analysis.

[c] Dispersion of the metallic phase, from SAXS measurements.

[d] Obtained by the equation $t = [(1 - Q)(1 - C_{1,3}) - Q \ln C_{1,3}]/K$, by fitting the experimental data (t vs $C_{1,3}$) using Q and K as nonlinear parameters. $C_{1,3}$ is the concentration of 1,3-COD. k_1 is in min^{-1}, Q is the ratio between the adsorption constant of COE and the adsorption constant of 1,3-COD on the catalyst surface.

[e] Turnover frequency (s^{-1}), calculated from $TOF_1 = (k_1 \times 10{,}000)/(60 \times D_x)$.

[f] k_2 is the rate constant in min^{-1} of the COE to cyclooctane (COA) hydrogenation, calculated from the initial slope.

[g] $S_{90} = \dfrac{\text{mol COE}}{\text{mol 1,3-COD converted}}$ % at 90% conversion.

[h] $S_{100} = \dfrac{\text{mol COE}}{\text{mol 1,3-COD converted}}$ % at 100% conversion.

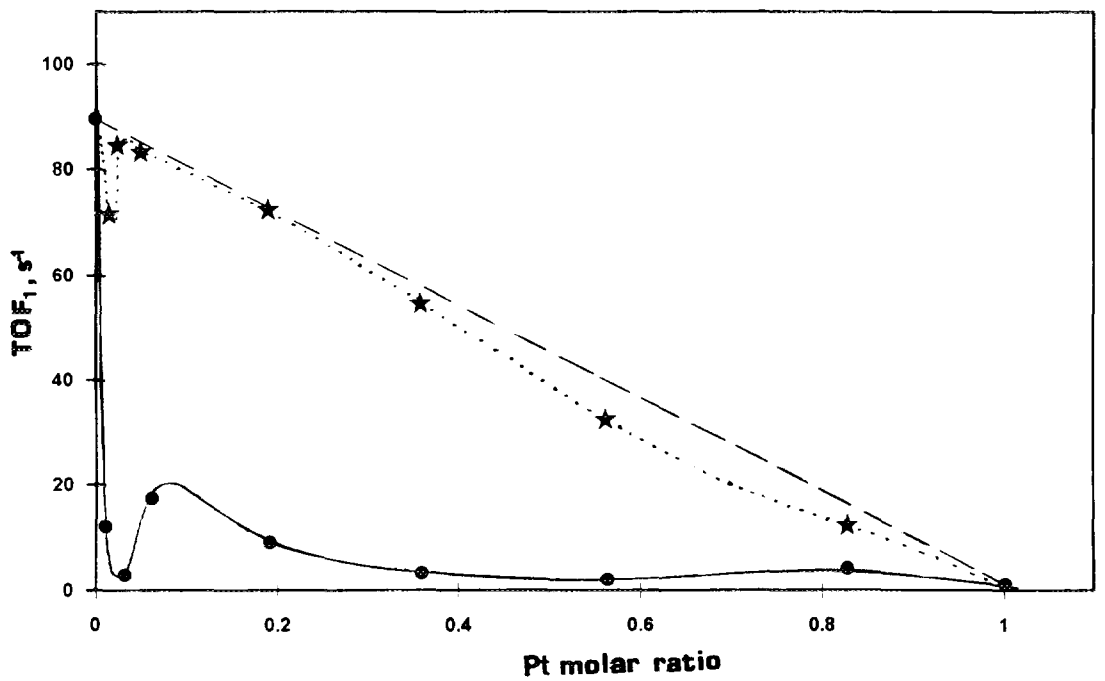

FIG. 3. Catalytic activity of pumice-supported Pd–Pt catalyst (TOF_1 vs content of Pt). The dotted line represents the turnover frequency expected for a mechanical mixture of the Pd_{100} and Pt_{100} catalysts used in this work at the same composition of the alloyed catalysts. The dotted line (★) represents the turnover frequency expected for a mechanical mixture of pure Pd and Pt catalysts having the same crystallite sizes and composition as those found in the alloyed catalysts.

the case of Pd on pumice the TOF_1 changes with the dimensions of crystallites and therefore the above curve is modified. It appears that a maximum is expected for the alloyed catalysts at about 90% Pd content.

Selectivity, which was practically 100% at 100% conversion with Pd/pumice catalysts, slightly decreases with the increase of the content in platinum of the bimetallic catalysts (Table 2). Since platinum shows a lower selectivity than palladium in the hydrogenation of 1,3-COD (23), the decrease in activity could be anticipated for Pd–Pt catalysts. The trend of S_{90} (Table 2) shows that the formation of the alloy does not give any particular change in selectivity, suggesting that the two metals maintain their own ensembles (29).

Our results are unattractive especially if compared with an increase of catalytic activity (with a maximum at ~90% Pd), reported in the liquid-phase hydrogenation of phenylacetylene with Pd–Pt alloy catalysts on vitreous supports (31). However, in that work the activity of the pure Pd catalyst was about twice that of the pure Pt one, whereas the activity of our pure Pd catalyst is about two orders of magnitude higher than that of our pure Pt catalyst. We believe that it is not coincidental that also in the case of Ref. (31) the maximum in activity corresponds to the catalyst at the lowest dispersion of the series of bimetallic samples investigated (41). When we performed the liquid-phase hydrogenation of phenylacetylene in the same operating conditions (49) as in this work, we found an activity for the pure Pd/pumice catalyst about 60 times higher than that found with the best Pd–Pt catalyst of Ref. (31). Finally, hydrogenation of 1,3-COD with our Pd–Pt catalysts under the same conditions but with magnetic stirring shows a similar trend as in Ref. (31) (Fig. 4). Although we have no data of TOF_1 for the hydrogenation of 1,3-COD with pure Pd/pumice catalysts using magnetic stirring, the maximum in Fig. 4, similarly to what was found in Fig. 3, could be due to the difference of activity manifested at different metal dispersions. In any case it is now evident that magnetic stirring does not overcome diffusion control phenomena. Obviously the diffusion limitations are more important when very active catalysts are used (50).

In principle both structural and electronic effects can be invoked to explain the decrease of activity and selectivity of the bimetallic catalysts. The reduced activity of platinum and the reduced amount of the Pd_4 units probably necessary for the surface reaction must be considered. Moreover, an increase in the nearest neighbour bond distance is expected as a consequence of the increase of the lattice parameters for Pd–Pt alloys. However, these effects, even added to segregation, are insufficient to explain the large decrease in activity documented also at very low percentage of platinum in the alloyed Pd–Pt catalysts. Pumice-supported Pd, Pt, and Pd–Pt

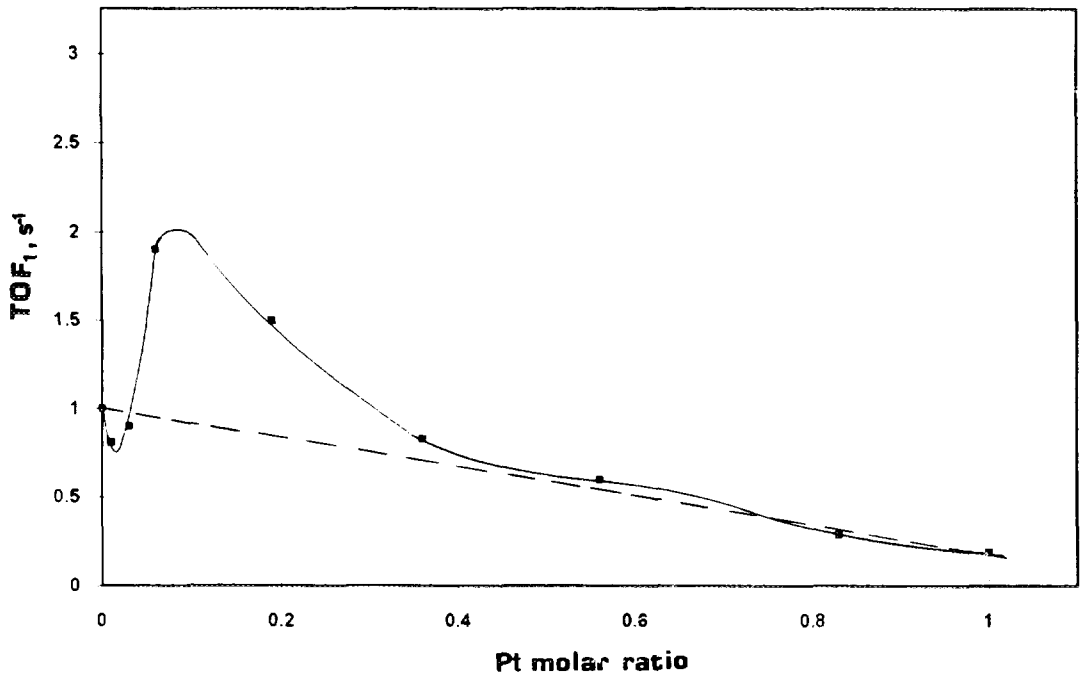

FIG. 4. Hydrogenation of 1,3-COD with magnetic stirring (TOF_1 vs content of Pt). The dotted line represents the turnover frequency expected for a mechanical mixture of the Pd_{100} and Pt_{100} catalysts used in this work at the same composition of the alloyed catalysts. The dimensions of the mixed crystallites are those of Pd_{100} and Pt_{100}.

catalysts were shown to shift the binding energy of the metal important orbitals towards lower values (9) indicating a decreased bonding of the electron-rich diolefin to pumice-supported metals. This effect should maintain the high rate of hydrogenation also when the dispersion of the metallic phase is large through a counterbalancing (8) of the loss of metallic character of the small metal crystallites. However, since the strength of metal–diolefin bonds is greater for platinum than for palladium, the various units containing Pt, like $PtPd_3$, Pt_2Pd_2, and Pt_3Pd, should give reaction intermediates more stable than the Pd_4 units. Evidently the electronic density transfer to pumice Pd–Pt supported catalysts is not sufficient to decrease the strength of the Pt–diolefin bond, thus explaining the progressive decreased activity as the content of platinum, in the alloyed catalysts, increases. As pointed out by a referee, in the hydrogenation of highly unsaturated hydrocarbons the decrease in activity in alloyed Pd–Pt catalysts could be expected, as well as a decrease of the selectivity (S = 100% in the palladium catalysts) owing to the addition of a metal, platinum, of known lower activity and selectivity in these reactions. Our results at least demonstrate that the claimed beneficial effects (31) of alloying platinum to palladium are incorrect.

5. CONCLUSIONS

The above characterization of pumice-supported Pd–Pt catalysts has shown some interesting structural results which can be summarized as follows: formation of alloyed crystallites at any Pd/Pt atomic ratio, high dispersion of the bimetallic clusters, and segregation onto the metal surface of the less abundant metal. The tests of activity of these catalysts in the liquid-phase hydrogenation of 1,3-COD have shown a negative effect of the addition of platinum to pumice-supported palladium catalysts. Both structural and electronic effects must be invoked to account for the reduced activity.

Since hydrogen diffusion may become a rate-determining step in liquid-phase hydrogenations when magnetic stirring and very active catalysts are employed, our results suggest that previous reports of improvement in activity (31) with supported Pd–Pt catalysts in the liquid-phase hydrogenation of highly unsaturated hydrocarbons, might be due to the presence of diffusion phenomena.

ACKNOWLEDGEMENTS

This work was supported by C.N.R. (Progetti Finalizzati Chimica Fine II and Materiali Speciali) and by the Ministero della Ricerca Scientifica e Tecnologica. We thank Pumex SpA for supplying samples of pumice and for a research grant to D. D.

REFERENCES

1. Bond, G. C., *Acc. Chem. Res.* **26,** 490 (1993); Bond, G. C., and Wells, P. B., *Adv. Catal.* **15,** 92 (1964).
2. Boitiaux, J. P., Cosyns, J., Derrien, M., and Leger, G., *Hydrocarbon Process.* **64,** 51 (1985).
3. Derrien, M. L., *in* "Catalytic Hydrogenation" (L. Červeny, Ed.), p. 613. Elsevier, Amsterdam, 1986.
4. Tardy, B., Noupa, C., Leclercq, C., Bertolini, J. C., Hoareau, A., Treilleux, M., Faure, J. P., and Nihoul, G., *J. Catal.* **129,** 1 (1991).
5. Sárkány, A., Weiss, A. H., and Guczi, L., *J. Catal.* **98,** 550 (1986).
6. Boitiaux, J. P., Cosyns, J., and Vasudevan, S., *in* "Preparation of Catalysts, III" (G. Poncelet, P. Grange, and P. A. Jacobs, Eds.), p. 123. Elsevier, Amsterdam, 1983.
7. Boitiaux, J. P., Cosyns, J., and Vasudevan, *Appl. Catal.* **6,** 41 (1983).
8. Deganello, G., Duca, D., Martorana, A., Fagherazzi, G., and Benedetti, A., *J. Catal.* **149,** 127 (1994).
9. Venezia, A. M., Duca, D., Floriano, M. A., Deganello, G., and Rossi, A., *SIA, Surf. Interface Anal.* **19,** 548 (1992).
10. Venezia, A. M., Duca, D., Floriano, M. A., Deganello, G., and Rossi, A., *SIA, Surf. Interface Anal.* **18,** 619 (1992).
11. Venezia, A. M., Floriano, M. A., Deganello, G., and Rossi, A., *SIA, Surf. Interface Anal.* **18,** 532 (1992).
12. Floriano, M. A., Venezia, A. M., Deganello, G., Svensson, E. C., and Root, J. H., *J. Appl. Cryst.* **27,** 271 (1994).
13. Matyi, R. J., Schwartz, L. H., and Butt, J. B., *Catal. Rev.–Sci. Eng.* **29,** 41 (1987).
14. Noakes, G. E., and Allin, E. J., *Can. J. Phys.* **31,** 40 (1953).
15. Fagherazzi, G., Benedetti, A., Martorana, A., Duca, D., and Deganello, G., *Catal. Lett.* **6,** 263 (1990).
16. Martorana, A., Deganello, G., Duca, D., Benedetti, A., and Fagherazzi, G., *J. Appl. Cryst.* **25,** 31 (1992).
17. Fagherazzi, G., Benedetti, A., Deganello, G., Duca, D., Martorana, A., and Spoto, G., *J. Catal.* **149,** 117 (1994).
18. Jolly, P. W., *Angew. Chem. Int. Ed.* **24,** 283 (1985).
19. Yermakov, Yu. I., *Catal. Rev.* **13,** 77 (1986).
20. Carturan, G., and Strukul, G., *J. Catal.* **57,** 516 (1979).
21. Cocco, G., Fagherazzi, G., Carturan, G., and Gottardi, V., *J. Chem. Soc., Chem. Commun.*, 979 (1978).
22. Becconsall, J. K., Job, B. E., and O'Brien, S., *J. Chem. Soc. (A),* 423 (1967).
23. Deganello, G., and Duca, D., unpublished results.
24. Pitchai, R., Wong, S. S., Takahashi, N., Butt, J. B., Burwell, R. L., and Cohen, J. B., *J. Catal.*, **94,** 478 (1985).
25. Sinfelt, J. H., "Bimetallic Catalysts: Discoveries, Concepts and Application." Wiley, New York, 1983.
26. Aduriz, R. H., Bodnariuk, P., Coq, B., and Figueras F., *J. Catal.* **129,** 47 (1991).
27. Peterson, J. R., *in* "Hydrogenation Catalysts," p. 183. Noyes Data Corp., Park Ridges, NY, 1977.
28. Palczewska, W., Jablonski, A., Kaszkur, Z., Zuba, G., and Wernish, J., *J. Mol. Catal.* **25,** 307 (1984).
29. Guczi, L., and Schay, Z., *in* "Catalytic Hydrogenation" (L. Červeny, Ed.), p. 313. Elsevier, Amsterdam, 1986.
30. Völter, J., *in* "Catalytic Hydrogenation" (L. Červeny, Ed.), p. 337. Elsevier, Amsterdam, 1986.
31. Carturan, G., Cocco, G., Facchin, G., and Navazio, G., *J. Mol. Catal.* **26,** 375 (1984).
32. Enzo, S., Polizzi, S., and Benedetti, A., *Kristallogr.* **170,** 275 (1985).
33. Benedetti, A., Cocco, G., Enzo, S., Pinna, F., and Schiffini, L., *J. Chem. Phys.* **78,** 875 (1981).

34. Polizzi, S., Benedetti, A., Fagherazzi, G., Franceschin, S., Goatin, C., Talamini, G., and Toniolo, L., *J. Catal.* **106,** 483 (1987).
35. Anderson, J. R., "Structure of Metallic Catalysts," p. 296. Academic Press, London, 1975.
36. Yoe, J. H., and Kirkland, J. J., *Anal. Chem.* **26,** 1335 (1954).
37. Boudart, M., and Hwang, H. S., *J. Catal.* **39,** 44 (1975).
38. Moraweck, B., Clugnet, G., and Renouprez, A., *J. Chem. Phys.* **83,** 265 (1986).
39. Bonivardi, A. L., and Baltanas, M. A., *J. Catal.* **138,** 500 (1992).
40. Fagherazzi, G., and Benedetti, A., unpublished results.
41. Cocco, G., Carturan, G., Enzo, S., and Schiffini, L., *J. Catal.* **85,** 405 (1984).
42. Scofield, J. K., *J. Electron Spectrosc. Relat. Phenom.* **8,** 129 (1976).
43. Reilman, R. F., Msezane, A., and Manson, S. T., *J. Electron Spectrosc. Relat. Phenom.* **8,** 389 (1976).
44. Seah, M. P., and Dench, W. A., *SIA, Surf. Interf. Anal.* **1,** 2 (1979).
45. Kujers, F. J., Tieman, B. M., and Ponec, V., *Surf. Sci.* **75,** 657 (1980).
46. Guczi, L., and Karpinski, Z., *J. Catal.* **56,** 438 (1979).
47. Happel, J., and Sellers, P. H., *Adv. Catal.* **32,** 273 (1983).
48. Rideal, E. K., *in* "Concepts in Catalysis," Academic Press, London/New York, 1968.
49. Duca, D., Liotta, L. F., and Deganello, G., *J. Catal.*, accepted for publication.
50. Gut, G., Kut, O. M., Yuecelen, F., and Wagner, D., *in* "Catalytic Hydrogenation" (L. Červeny, Ed.), p. 517. Elsevier, Amsterdam, 1986.